Unmanned Aerial Vehicle Propeller Noise

Kingan, Michael J.; McKay, Ryan S.; Wu, Yan; Jung, Riul; Go, Sung Tyaek

DOI
10.1007/978-3-031-73935-4_6

Publication date
2025

Document Version
Final published version

Published in
Flinovia-Flow Induced Noise and Vibration Issues and Aspects-IV

Unmanned Aerial Vehicle Propeller Noise

Michael J. Kingan, Ryan S. McKay, Yan Wu, Riul Jung, and Sung Tyaek Go

Abstract This paper gives an overview of work investigating the noise produced by the propellers used on small multi-rotor unmanned aerial vehicles (UAVs) which has been recently undertaken at the University of Auckland. There are a number of different physical mechanisms by which these propellers generate noise and these have been studied using computational and analytical modelling and experimental measurements. Sources of noise which are covered in this paper are: steady loading and thickness noise sources for isolated and shrouded propellers; unsteady blade motion; turbulent inflow for isolated and shrouded propellers; unsteady loading due to propeller-strut interaction; and the unsteady loading on the blades of a contra-rotating propeller. The paper also describes some recent work undertaken to develop a standardised method for measuring noise from UAVs which includes assessing the suitability of ground-board mounted microphones for outdoor noise measurements and identifying appropriate metrics for quantifying UAV noise. The paper concludes with suggestions for future work.

Keywords Unmanned aerial vehicles · Propeller noise · Turbulent inflow noise

M. J. Kingan (✉) · S. T. Go
Acoustics Research Centre, Department of Mechanical and Mechatronics Engineering, The University of Auckland, Auckland, New Zealand
e-mail: m.kingan@auckland.ac.nz

R. S. McKay
Dotterel Technologies Ltd., Auckland, New Zealand

Y. Wu
Section Wind Energy, Faculty of Aerospace Engineering, Delft University of Technology, Delft, The Netherlands

R. Jung
Acoustics Research Centre, University of Salford, Salford, UK

C. Doolan et al. (eds.), *Flinovia—Flow Induced Noise and Vibration Issues and Aspects—IV*, https://doi.org/10.1007/978-3-031-73935-4_6

1 Introduction

Multi-rotor unmanned aerial vehicles (UAVs) are becoming more prevalent and these aircraft can produce noise that impacts humans and animals where they operate. These small aircraft typically have four, six, or eight single or coaxial propellers/rotors with fixed pitch blades which are driven by electric motors. The thrust and torque produced by each rotor is varied by changing the rotor speed. For most configurations, during hover, the rotor axes are aligned near-vertically, but during horizontal flight, the rotor axes are tilted with the body of the UAV.

The noise generated by a multi-rotor UAV is primarily produced by aeroacoustic sources generated by the rotors, but there can be some contribution from the electric motors [1]. Despite propeller and helicopter rotor noise being the subject of many decades of investigation, the dominant mechanisms by which the noise from a UAV is generated are not well understood. These need to be identified and noise prediction methods developed to enable lower-noise UAVs to be designed. In addition to this, studying the noise produced by small UAVs is a good precursor to studying the noise from larger UAVs and the small VTOL aircraft which are anticipated to become more prevalent in coming years which will have stringent noise regulations to comply with.

2 Noise from Isolated Propellers

Work to investigate the noise produced by UAV propellers started at the University of Auckland in 2016. Preliminary experiments involved mounting a single propeller on a pole within a 5.3 m $\times$ 5.3 m $\times$ 5.3 m anechoic chamber as shown in Fig. 1 which presents photographs showing the experimental set-up. The electric motor was enclosed in a steel housing to eliminate noise from the electric motor. A laser Doppler vibrometer scan was used to confirm that the noise radiated from the surface of the motor enclosure was negligible [1]. The rig was mounted on an S-beam load cell to measure the thrust during operation and an array of ½″ microphones mounted on a C-shaped support structure were used to measure the radiated noise field. Note that the support structure was lagged with sound absorbing material to reduce the effect of reflections from the structure itself.

Figure 2 presents the measured narrowband sound pressure level spectra produced by a 15″ diameter T-motor propeller generating 12 N of thrust. The polar angles of the microphones used for each measurement are indicated above each subplot (refer to Fig. 1 to see these locations relative to the propeller). These spectra show a multitude of tones at harmonics of the blade passing frequency (BPF) at all positions, including on-axis. The causes of these tones were not understood, but several possible sources were hypothesized. These included: steady loading and thickness noise sources, turbulent inflow noise caused by turbulence within the anechoic chamber, unsteady rotational motion of the rotor blades, and blade flutter/vibration.

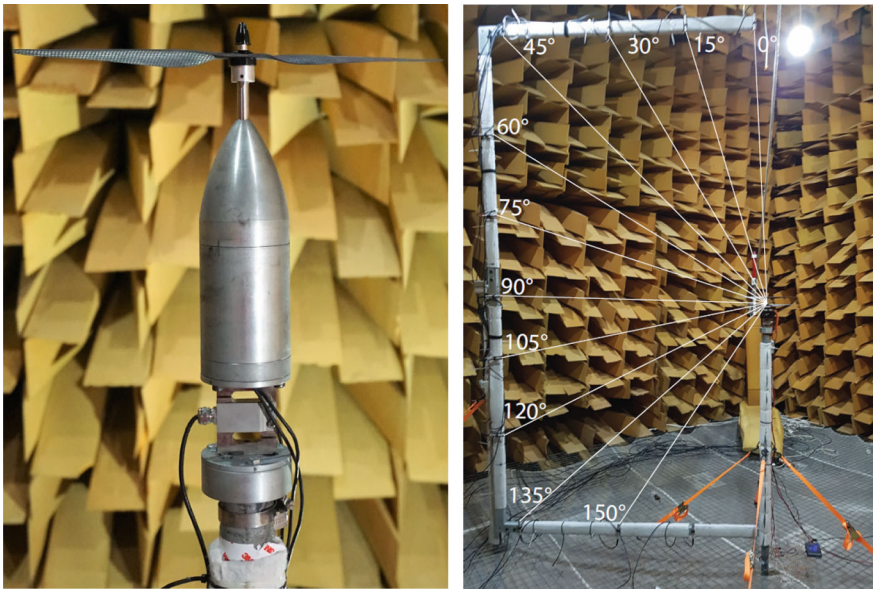

Fig. 1 Photographs of the propeller test-rig mounted in the anechoic chamber. Close-up photograph showing the rig with motor enclosure and load cell (left). Photograph showing the test-rig and surrounding microphone array (right)

2.1 Steady Loading and Thickness Tones

The thickness of, and steady loading on, the surface of the propeller blades produces a pressure perturbation within the surrounding air which rotates with the propeller. In a fixed frame of reference, this pressure perturbation is periodic and thus has a spectrum which consists of tones at harmonics of the blade passing frequency. Each tone has the form of a cylindrical harmonic which rotates at the speed of the propeller. The pressure field of each tone decays evanescently until the sonic radius at which point it propagates efficiently.

Steady loading tones can be predicted accurately and straightforwardly once the steady loading distribution on the propeller blades is determined. This can be estimated using simple blade element methods or Reynolds-averaged Navier Stokes (RANS) computational fluid dynamics (CFD) simulations. An acoustic analogy method can then be used to predict the radiated acoustic pressure field. A time-domain method, such as Farassat's formulation 1A [2], or a frequency-domain method, such as that described by Hanson and Parzyck [3] can be used for this purpose. Predictions made using such an approach (and reported in [4]) showed that for a 15″ diameter T-motor propeller operating in the hover condition, the steady loading and thickness sources only made a significant contribution to the first tone at the BPF over a wide range of polar angles, and the second and third BPF harmonic tones at observer locations close to the plane of rotation of the propeller. Thus, in the spectra presented in

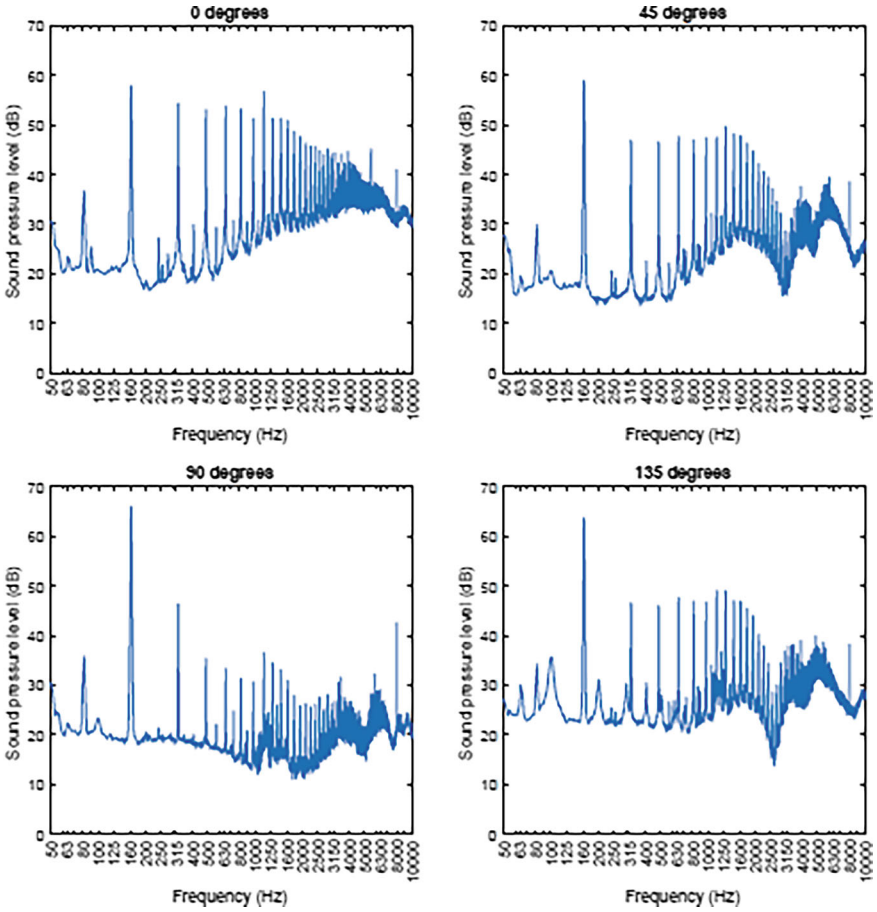

Fig. 2 Narrowband sound pressure level spectra produced by a 15″ diameter T-motor propeller generating 12 N of thrust. The polar angles for each measurement are indicated in the subplot titles and all measurements have been corrected to a constant observer radius assuming spherical spreading

Fig. 2, the large number of high frequency tones, and the tones which radiate along the propeller axis, must be caused by other mechanisms.

As an alternative to predicting the steady loading and thickness tones numerically, a method was developed by Wu et al. [4] for making high fidelity measurements of the 'steady rotational pressure field' surrounding the propeller. This involved using a traversing probe microphone to measure the pressure at a series of points along a line outboard of the propeller tip and parallel to the propeller axis (see Fig. 3). A quadrature encoder was attached to the propeller and at each measurement location the measurement was ensemble averaged over many rotations to produce a mean fluctuating pressure field at that point—which corresponded to the mean pressure

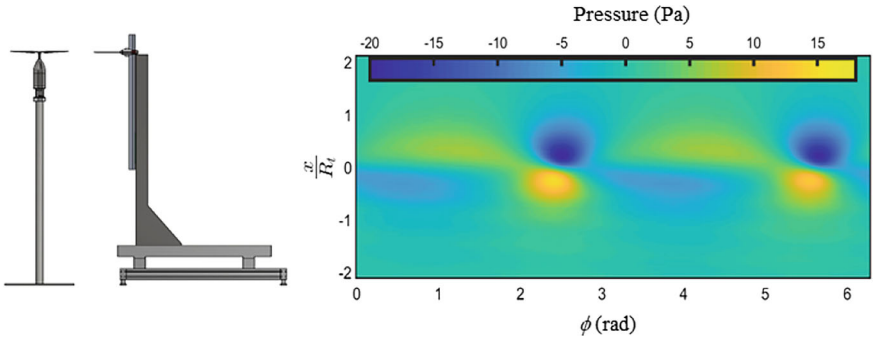

Fig. 3 Schematic showing a UAV propeller mounted on a pole with a traversing probe microphone adjacent (left). Ensemble-average pressure field on a cylindrical surface surrounding the propeller (right)

field which rotated with the propeller. By taking many measurements along a line, an image of the rotating acoustic pressure field on a cylindrical surface surrounding the propeller could be generated. An example of such an image is shown in Fig. 3. This high-fidelity pressure field can then be projected to the acoustic far-field using a method similar to cylindrical acoustic holography.

2.2 Unsteady Rotational Speed as a Noise Source

The source of the high frequency tones observed in Fig. 2 was unknown. We hypothesized that one possible source of this noise was the unsteady rotational motion of the propellers caused by the electric motors which drive the propellers. In order to test this hypothesis, we developed a noise prediction method which is described briefly here and more fully in Ref. [5]. Firstly, the time variation of rotor blade position was measured using a quadrature encoder. This data was used to calculate the rotational speed of the propeller as a function of time. A form of unsteady two-dimensional aerofoil theory known as arbitrary motion theory [6] was used to estimate the loading along the span of each propeller blade and the radiated acoustic pressure was calculated using Farassat's formulation 1A [2]. Predictions made using this method showed reasonable agreement with measurements of the half BPF harmonics (1.5 $\times$ BPF, 2.5 $\times$ BPF, etc.) for some cases.

There have been subsequent studies investigating this noise generation mechanism [7, 8]. We intend to investigate this noise source further in order to assess the importance of this source for a variety of different propellers and electric motors and to understand the cause of the unsteady motion.

2.3 *Flow Recirculation/Turbulent Inflow Noise*

Weitsman et al. [9] showed that a UAV propeller operated within a closed anechoic chamber (measuring 3.25 m × 2.55 m × 3.86 m) produced significant unsteady loading and a multitude of tones at harmonics of the BPF which only occurred several seconds after the propeller was started and reached its operating speed. The sound pressure level of the tones at the measurement positions was also observed to fluctuate with time. We repeated this experiment in the larger anechoic chamber at the University of Auckland (which measures 6 m × 6 m × 6 m) [5]. We also observed a multitude of tones at harmonics of the BPF in our measured sound pressure level spectra. However, these tones occurred immediately once the propeller started, and the level of the tones appeared to be relatively constant with time in comparison to those observed by Weitsman et al.

We also measured the sound pressure level spectrum produced by a 15″ diameter T-motor propeller mounted on a pole outdoors above a flat grass-covered field during very calm atmospheric conditions. The spectra measured outdoors are compared with those measured inside the anechoic chamber in Fig. 4 at a polar angle of 0° (i.e. directly above the propeller). The spectra are qualitatively similar and both contain a multitude of tones at harmonics of the blade passing frequency. Tones are also observed at intermediate frequencies. These could be caused by differences between the propeller blades or possibly the unsteady blade motion noise source. An exact match between the measurements is not expected as the outdoor measurements are affected by ground reflections. The turbulent inflow onto the propeller in both cases was also likely somewhat different.

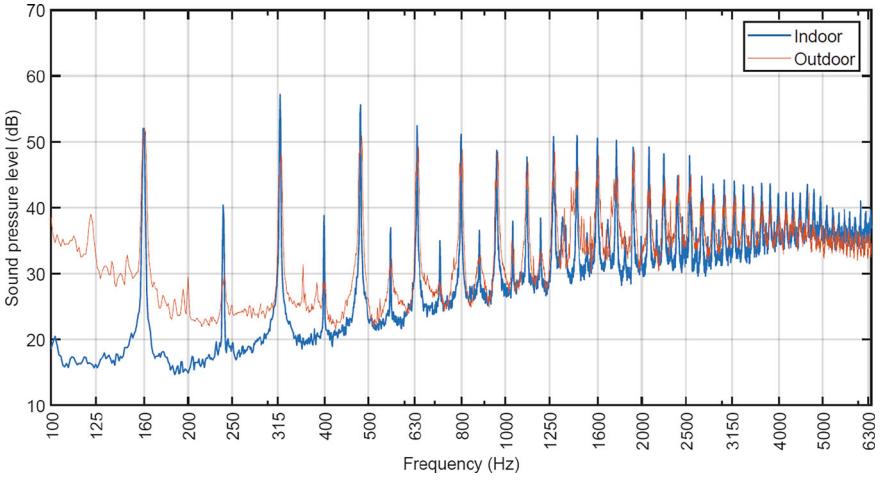

Fig. 4 Narrow-band sound pressure level spectra produced by a single 15″ diameter T-motor propeller mounted on a pole and operating in a hover condition. Measurement conducted in an anechoic chamber (blue); measurement conducted outdoors above a flat grass-covered field (orange)

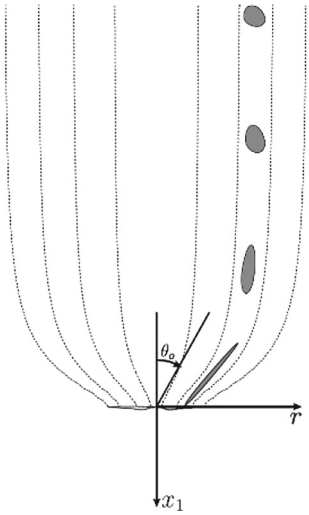

Fig. 5 Schematic showing the stream tube contraction through a propeller and the distortion of a turbulent eddy

A UAV propeller operating in hover 'sucks' in turbulence in the air above the propeller. The strong streamtube contraction produced when the propellers operate in hover causes the turbulent eddies incident onto the propeller to be elongated. This process is illustrated in Fig. 5. These elongated turbulent eddies are cut many times by the propeller blades—producing correlated unsteady loading on the propeller blades and thus 'quasi-tonal' noise.

In order to predict the noise produced by this source, models for several physical mechanisms are required. Firstly, the inhomogeneous, anisotropic turbulence just upstream of the propeller needs to be predicted. Secondly, the unsteady loading on the propeller blades caused by their interaction with the turbulence needs to be calculated. Finally, the radiated noise due to this unsteady loading can be computed. There are several models that have been developed following this general approach, and we decided to implement a model similar to that developed by Majumdar and Peake [10] and Robison and Peake [11]. In these methods, the flow distortion produced by the propeller is modelled using an actuator disc method and rapid distortion theory is used to calculate how this flow distortion modifies the characteristics of the incident flow field. We have used hot-wire measurements to tune this model so that the characteristics of the turbulence incident on a propeller operating in our anechoic chamber is a good match to that used in the model. The unsteady blade loading response to a turbulent gust is calculated using standard isolated blade response functions and then the radiated acoustic field is calculated using a frequency-domain approach.

Noise calculations made using this method are computationally very demanding, and therefore an alternative simplified method has also been developed which can be evaluated much more quickly. In this method, the propeller is modelled as being immersed in a uniform mean flow with turbulence which is anisotropic. A suitable turbulence model for such a case is the axisymmetric Kerschen-Gliebe spectrum

[12, 13] which requires the mean-square velocity and integral length scales in the axial and transverse directions to be specified. Further simplifications, which further reduce the computational time, can be made for an observer which is located on the propeller axis and for the case where the unsteady loading on the propeller is dominated by the axial component. The resulting expressions can be evaluated very rapidly and are well-suited to performing parametric investigations. We intend to publish a paper describing these methods soon.

Sample predictions made using these methods are shown in Figs. 6 and 7. Figure 6 plots the narrowband sound pressure level spectrum predicted at an observer located on the propeller axis produced by a 15″ diameter propeller operating in the hover condition. It is observed that the spectrum contains a multitude of 'quasi-tonal' humps centred on the harmonics of the BPF. Integrated noise levels for each hump are also shown. Although the measured and predicted spectra are qualitatively similar, the predicted levels are significantly lower than the measured levels. Figure 7 compares the sound pressure level (SPL) directivity at frequencies corresponding to the first four BPF harmonics. The predicted directivity patterns of the SPL at the 2nd, 3rd, and 4th BPF harmonics capture the shape of the measured data, but the levels are underpredicted. The disagreement between the measured and predicted levels at the BPF is due to the steady loading and thickness noise dominating the radiated sound field at most observer locations at this frequency.

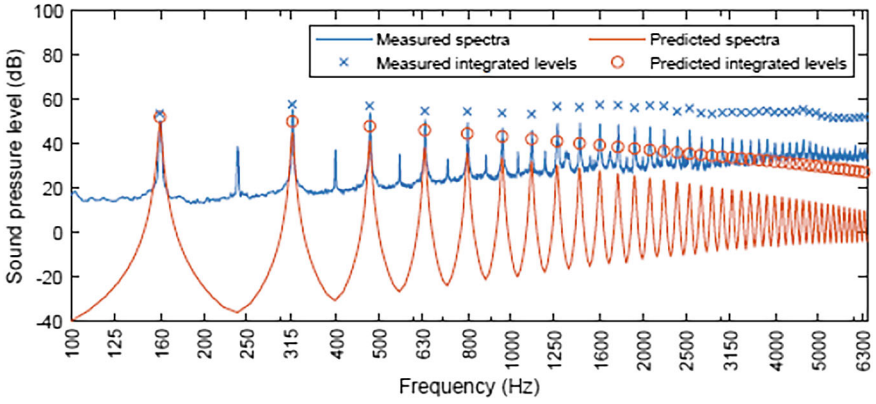

Fig. 6 Comparison between predictions and measurements of the sound pressure level spectrum measured/predicted at an observer located on the propeller axis for a 15″ diameter propeller rotating at 500 rad s^{-1}. The integrated levels were calculated by integrating the power spectral density over each 'hump' centred at the BPF and its harmonics

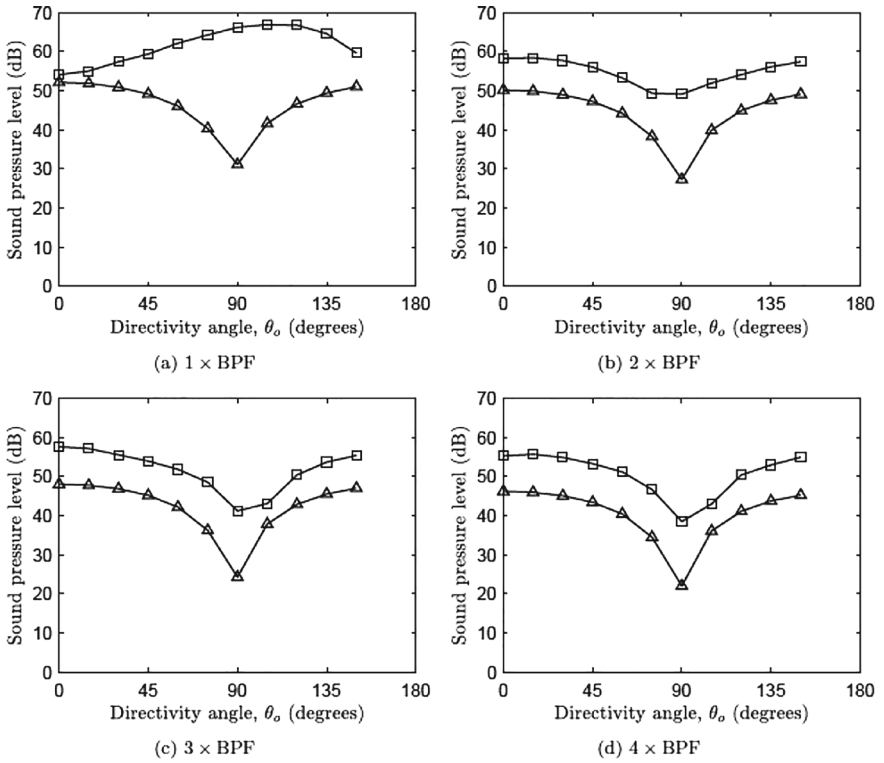

Fig. 7 SPL directivity patterns at different frequencies predicted for a 15″ diameter propeller operating in a hover condition. Measured (squares), predicted (triangles)

3 Noise from Shrouded Propellers

3.1 Turbulent Inflow Noise

We have extended the turbulent inflow noise model to include the effect of a shroud [14, 15]. This extension requires that the effect of the shroud on the mean-flow (and thus the turbulence distortion) and the acoustic shielding provided by the shroud is taken into account. The mean-flow model uses an actuator disc to represent the propeller and a panel method to model the effect of the shroud. The acoustic scattering from the shroud is calculated using a boundary element method. This approach allows the acoustic effect of lining the inner surface of the shroud to be taken into account.

This method was validated using experimental data collected in the anechoic wind tunnel at the University of Bristol. Photographs showing the experimental setup are shown in Fig. 8. Acoustic measurements were made using a polar array of microphones located outside the air stream. A turbulence grid was installed just upstream of the exit jet which was used to generate a turbulent inflow onto the propeller. The

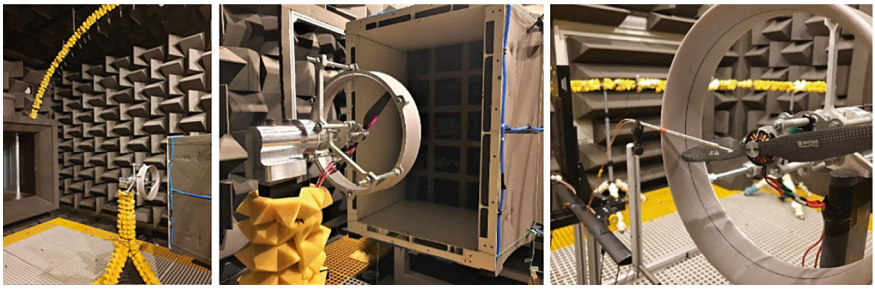

Fig. 8 Photographs showing testing of a shrouded UAV propeller being tested in the anechoic wind tunnel at the University of Bristol. Looking downstream towards the rig with the microphone array overhead (left). Looking upstream into the wind tunnel exit with turbulence grid installed (middle). Closeup showing a hotwire probe mounted in front of the propeller (right)

turbulent inflow was characterised using hotwire measurements made just upstream of the propeller. Figure 9 shows an example prediction of the polar directivity at four different frequencies compared with measurements for the shrouded and unshrouded propellers operating in the turbulent inflow. The predictions capture the general directivities measured in the experiments.

3.2 Steady Loading and Thickness Tones

A shroud also affects the steady loading and tonal noise produced by the propeller operating in the hover condition. The shroud has a curved inlet which produces a region of low pressure adjacent to this surface which generates a significant amount of thrust. This reduces the loading on the propeller blades which reduces the steady loading tones radiated from the propeller itself. However, loading sources are generated on the inner surface of the shroud which rotate with the propeller and produce tonal noise. We have recently developed a method [16] for measuring the loading sources on the inner surface of a UAV propeller shroud using a probe microphone. This involved drilling a number of holes into the side of a solid shroud into which the probe microphone was inserted so that its tip was flush with the inner surface of the shroud. A quadrature encoder was attached to the motor which was used to determine the angular position of the propeller during testing. Each probe microphone measurement was then ensemble averaged over many revolutions of the propeller to provide an estimate of the average pressure on the inner surface of the shroud rotating with the propeller. Multiple measurements were used to build up a picture of the pressure field on the entire inner surface of the shroud which is shown in Fig. 10. The measured pressure field compared very well with data from a RANS CFD simulation.

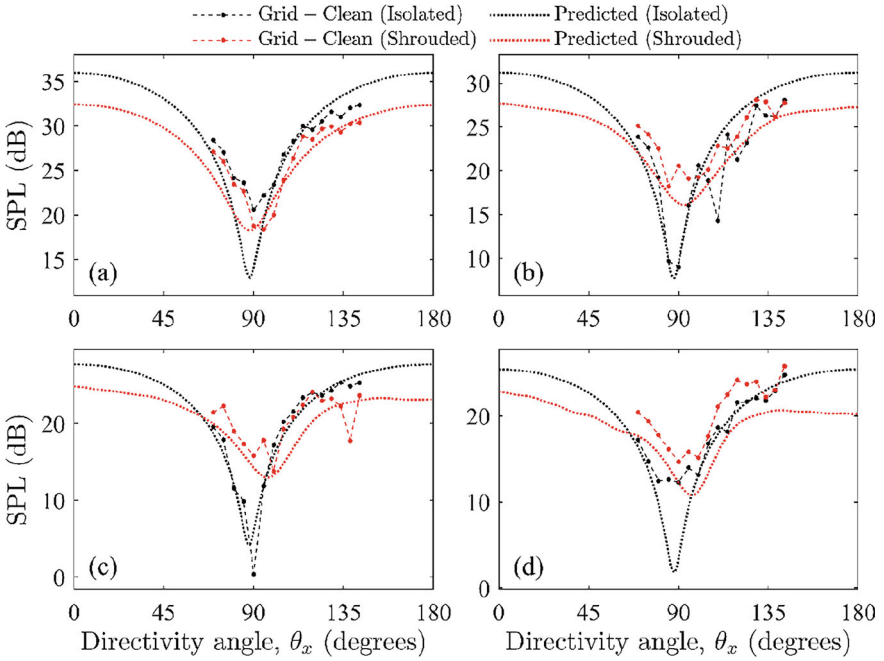

Fig. 9 Sound pressure level polar directivity plots of the noise produced by the isolated propeller and shrouded propeller at the **a** 5th, **b** 10th, **c** 15th, **d** 20th BPF harmonics. 'Grid–Clean' refers to clean inflow measurements subtracted from grid inflow measurements

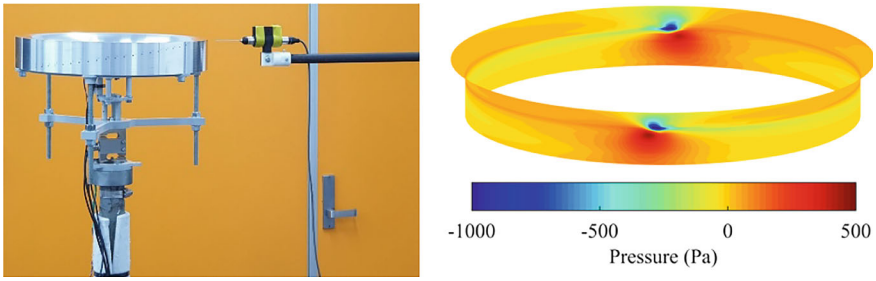

Fig. 10 Probe microphone measuring pressure on the inner surface of the shroud with a propeller operating inside (left). Image showing the measured pressure distribution on the inner surface of the shroud (right)

4 Propeller-Strut Interaction Noise

We have also investigated the noise produced when a straight circular strut is mounted adjacent to an operating propeller [17]. A visualization of the flow around such a configuration is shown in Fig. 11 which shows the tip vortex shed from the propeller

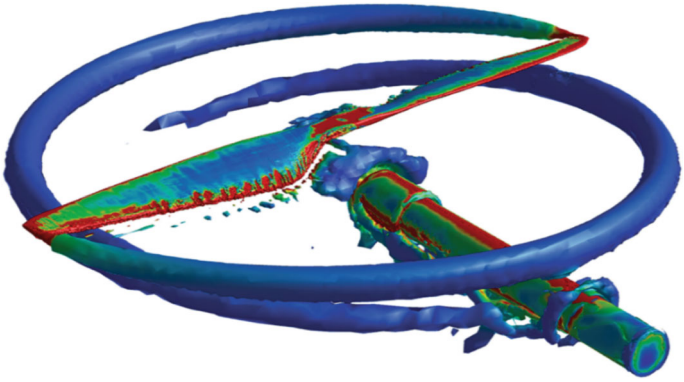

Fig. 11 Visualization of data from a CFD simulation of the flow around a propeller with a strut mounted 20 mm downstream showing isosurfaces of constant λ_2 criterion coloured by vorticity magnitude

tip interacting with the circular strut beneath the propeller. For this case, as the propeller blade passes the strut, impulsive loading is produced on the propeller blade and on the strut. This impulsive loading causes pressure impulses to radiate from both surfaces. In Ref. [17] it is shown that the directivity of the pressure impulses from the strut and propeller are quite different and thus the pressure impulses add together differently at different locations. An example showing how the pressure impulses radiated from the strut and propeller add together is shown in Fig. 12 which plots the pressure impulse at a particular far-field location versus non-dimensional time for a single propeller rotation. The plot separately shows the predicted pressure impulse produced by the sources on the propeller and the strut as well as the total pressure impulse. The total pressure impulse compares well with an experimental measurement conducted in the anechoic chamber at the University of Auckland.

5 Contra-Rotating Propeller Noise

Contra-rotating propellers are often used on UAVs to provide high thrust for a small planform area. A photograph of such a configuration is shown in Fig. 13. These rotors can produce significant noise levels due to the multitude of interaction tones caused by the periodic unsteady loading on the propeller blades produced when the blades pass each other [18]. Jung et al. [19] developed a frequency domain method which can be used to directly predict the radiated tonal sound pressure levels. The predictions require the unsteady loading on the blades of the propellers which can be calculated using an unsteady Reynolds-averaged Navier–Stokes (URANS) CFD simulation or using an analytical model. Such an approach was shown to produce predictions which were in excellent agreement with experimental measurements. This paper also demonstrated that for rotor configurations where the axial gap between the

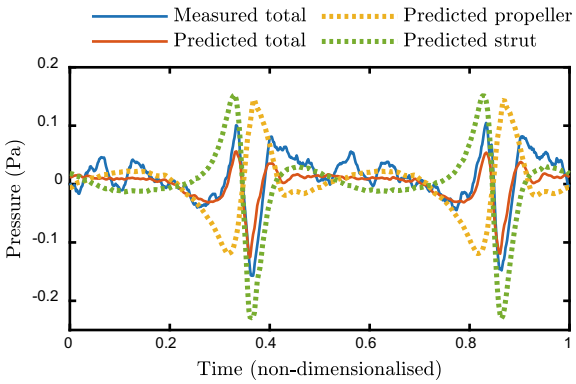

Fig. 12 Measured and predicted acoustic pressure impulse produced by a propeller-strut interaction versus non-dimensional time at a far-field location. Measured total pressure (blue solid line), predicted total pressure (orange solid line), predicted pressure radiated from the propeller (yellow dotted line), predicted pressure radiated from the strut (green dotted line)

Fig. 13 Photograph of a contra-rotating UAV rotor system with T-motor blades mounted in the anechoic chamber at the University of Auckland

propellers was small, the bound potential field produced by the rotors was the primary cause of the periodic unsteady loading on the propeller blades—and thus the radiated interaction tones. As the bound potential field decays rapidly away from the propeller, a simple method to reduce the noise level is to increase the axial gap between the propellers.

An alternative method of noise reduction was explored in Jung et al. [20] in which the rotor blades were skewed as shown in Fig. 14. The idea behind this concept is that the skewed blades on the top and bottom propellers pass over each other at different times along the blade span. This means that the acoustic pressure impulses produced by the unsteady loading along the blade span are de-phased when they

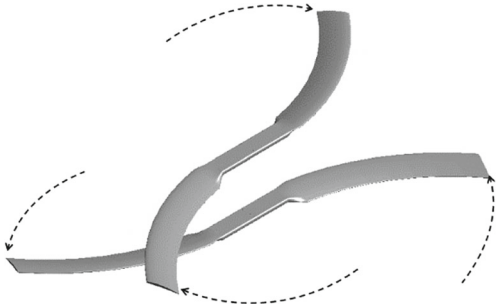

Fig. 14 Schematic of a contra-rotating UAV rotor system with skewed blades

arrive at the observer location. The experimental and numerical study reported in Ref. [20] confirmed that a contra-rotating propeller system with skewed blades produces significantly lower noise levels than an equivalent rotor with straight blades and that the de-phasing effect was partially responsible for this reduction.

6 Noise Metrics and Measurement Methods

Work is currently underway to develop an ISO standard which will specify methods for measuring the noise produced by small (<150 kg) 'unmanned aircraft systems'. This standard covers measurements to be made in anechoic chambers, anechoic wind tunnels and outdoors. In order to support the development of this standard, a study was conducted to investigate appropriate metrics for quantifying the noise produced by a UAV during flight [21]. The study made use of four different UAVs operating in hover or in straight and level flight. Measurements made using a ½″ microphone were used to calculate a range of different noise metrics for each noise event. Noise recordings were also made using a spherical microphone array. These noise recordings were reproduced using a 3D sound reproduction system as part of a series of subjective tests to determine the level of annoyance produced by each noise event. It was found that the maximum A-weighted sound pressure level correlated most strongly with the subjective annoyance ratings for flyby noise events, whereas the continuous A-weighted sound pressure level correlated best for hover noise events.

Further work needs to be undertaken to verify the reliability/repeatability and equivalence of the proposed noise measurement methods. In particular, the outdoor noise measurement method proposed in the standard utilises ground-board mounted microphones. Our recent study [22] has shown that sound pressure level measurements made using this microphone configuration are strongly dependent on the impedance of the surrounding ground, the frequency of the sound and the angle of incidence of the sound. Ideally, a noise level measurement would be independent of these parameters. It may be possible to develop corrections for these microphone measurements. Alternatively, another method of mounting the microphones during outdoor noise measurements should be developed.

7 Conclusions and Recommendations for Future Work

Work on the noise produced by UAV propellers has been conducted at the University of Auckland for the last eight years. We have explored many aspects of this noise and have developed methods to predict it and reduce it. It is difficult to believe that so much effort has been expended on a problem which seemed quite straightforward when we first delved into it! However, several questions remain unanswered, and there are still some aspects of UAV propeller noise which present interesting opportunities for research. In particular:

- Further work should be conducted to assess the importance of the noise produced by unsteady blade motion.
- The importance of flow recirculation within anechoic chambers of different sizes is unknown and should be investigated. This appears to be an important noise source in some chambers.
- The cause of turbulence in the flow recirculating within an anechoic chamber should be identified, so that controls can be developed.
- The effect of different strut geometries and surface treatments should be explored.
- The proposed standard methods for reliably measuring the noise levels produced by a UAV in flight outdoors need further development and investigation.

Acknowledgements The work described in this paper was supported by a number of different grants and mechanisms which are gratefully acknowledged and which are listed below. Ryan McKay and Riul Jung were partially funded by doctoral scholarships from Callaghan Innovation and supported by Dotterel Technologies Ltd. Ryan McKay and Sung Tyaek Go were supported by University of Auckland Doctoral Scholarships. Yan Wu, Ryan McKay and Riul Jung received support from the Acoustics Research Centre at the University of Auckland. Many of the computations described in this paper made use of the high performance computing resources provided by New Zealand's National e-Science Infrastructure (NeSI).

References

1. McKay, R.S., Kingan, M.J.: Multi-rotor unmanned aerial system noise: quantifying the motor's contribution. In: Proceedings of the Conference of the Acoustical Society of New Zealand (2018)
2. Brentner, K.S.: Prediction of Helicopter Rotor Discrete Frequency Noise: A Computer Program Incorporating Realistic Blade Motions and Advanced Acoustic Formulation, NASA TM 87721 (1986)
3. Hanson, D.B., Parzych, D.J.: Theory for Noise of Propellers in Angular Inflow with Parametric Studies and Experimental Verification, NASA CR 19930015905 (1993)
4. Wu, Y., Kingan, M.J., McKay, R.S., Go., S.T., Shim, Y.: Extrapolation and inversion of near-field propeller noise measurements. Appl. Acoust. **185**, paper no. 108395 (2022)
5. McKay, R.S., Kingan, M.J.: Multi-rotor unmanned aerial system propeller noise caused by unsteady blade motion. In: Proceedings of the 25th AIAA/CEAS Aeroacoustics Conference, paper no. 2499 (2019)

6. Van der Wall, B.G., Leishman, J.G.: The influence of variable flow velocity on unsteady airfoil behavior. J. Am. Helicopter Soc. **39**, 836–845 (1994)
7. Zhong, S., Zhou, P., Chen, W., Jiang, H., Wu, H., Zhang, X.: An investigation of rotor aeroacoustics with unsteady motions and uncertainty factors. J. Fluid Mech. **956**, paper no. A16 (2023)
8. Zhong, S., Zhou, P., Fattah, R., Zhang, X.: A revisit of the tonal noise of small rotors. Proc. R. Soc. A **476**, paper no. 2244 (2020)
9. Weitsman, D., Stephenson, J.H., Zawodny, N.S.: Effects of flow recirculation on acoustic and dynamic measurements of rotary-wing systems operating in closed anechoic chambers. J. Acoust. Soc. Am. **148**, paper no. 1325 (2020)
10. Majumdar, S.J., Peake, N.: Noise generation by the interaction between ingested turbulence and a rotating fan. J. Fluid Mech. **359**, 181–216 (1998)
11. Robison, R.A.V., Peake, N.: Noise generation by turbulence-propeller interaction in asymmetric flow. J. Fluid Mech. **758**, 121–149 (2014)
12. Kerschen, E.J., Gliebe, P.: Noise caused by the interaction of a rotor with anisotropic turbulence. AIAA J. **19**(6), 717–723 (1981)
13. Posson, H., Moreau, S., Roger, M.: Broadband noise prediction of fan outlet guide vane using a cascade response function. J. Sound Vib. **330**(25), 6153–6183 (2011)
14. Go, S.T., Kingan, M.J., McKay, R.S., Sharma, R.N.: Turbulent inflow noise produced by a shrouded propeller. J. Sound Vib. **542**, paper no. 117366 (2023)
15. Go, S.T., Kingan, M.J., Bowen, L., Azarpeyvand, M.: Noise of a shrouded propeller due to ingestion of grid-generated turbulence. J. Sound Vib. **571**, paper no. 118044 (2024)
16. Go, S.T. Kingan, M.J., Wu, Y., Sharma, R.N.: Experimental and numerical investigation of the sound field produced by a shrouded UAV propeller. Appl. Acoust. **211**, paper no. 109523 (2023)
17. Wu, Y., Kingan, M.J., Go., S.T.: Propeller-strut interaction tone noise. Phys. Fluids **34**, paper no. 055116 (2022)
18. McKay, R.S., Kingan, M.J., Go, S.T. Jung, R.: Experimental and analytical investigation of contra-rotating multi-rotor UAV propeller noise. Appl. Acoust. **177**, paper no. 107850 (2021)
19. Jung, R., Kingan, M.J., Dhopade, P., Sharma, R.N., McKay, R.S.: Investigation of the interaction tones produced by contra-rotating unmanned aerial vehicle rotor systems. AIAA J. **61**(7), 3142–3157 (2023)
20. Jung, R., Kingan, M.J., Dhopade, P., Sharma, R.N., McKay, R.S., Dai, Z, Symons, D., Pearse, J.: The effect of blade skew on the interaction tones produced by a contra-rotating unmanned aerial vehicle rotor system. J. Sound Vib. 118186 (2023)
21. Hui, C.T.J., Kingan, M.J., Hioka, Y., Schmid, G., Dodd, G., Dirks, K.N., Edlin, S., Mascarenhas, S., Shim, Y.: Quantification of the psychoacoustic effect of noise from small unmanned aerial vehicles. Int. J. Environ. Res. Public Health **18**(17), 8893 (2021)
22. Kingan, M.J., Go, S.T., Piscoya, R., Ochmann, M.: On the modelling of ground-board mounted microphones for outdoor noise measurements. J. Sound Vib., paper no. 117894 (2023)